

Nanoscale

Accepted Manuscript



This is an *Accepted Manuscript*, which has been through the Royal Society of Chemistry peer review process and has been accepted for publication.

Accepted Manuscripts are published online shortly after acceptance, before technical editing, formatting and proof reading. Using this free service, authors can make their results available to the community, in citable form, before we publish the edited article. We will replace this *Accepted Manuscript* with the edited and formatted *Advance Article* as soon as it is available.

You can find more information about *Accepted Manuscripts* in the [Information for Authors](#).

Please note that technical editing may introduce minor changes to the text and/or graphics, which may alter content. The journal's standard [Terms & Conditions](#) and the [Ethical guidelines](#) still apply. In no event shall the Royal Society of Chemistry be held responsible for any errors or omissions in this *Accepted Manuscript* or any consequences arising from the use of any information it contains.

Cite this: DOI: 10.1039/c0xx00000x

www.rsc.org/xxxxxx

ARTICLE TYPE

Controllable Conversion of Plasmonic Cu_{2-x}S Nanoparticles to Au₂S by Cation Exchange and Electron Beam Induced Transformation of Cu_{2-x}S/Au₂S Core/Shell Nanostructures

Xianliang Wang,⁺ Xin Liu,⁺ Dewei Zhu, and Mark Swihart^{*}⁵ These authors equally contributed to this work

Received (in XXX, XXX) Xth XXXXXXXXXX 20XX, Accepted Xth XXXXXXXXXX 20XX

DOI: 10.1039/b000000x

Self-doped Cu_{2-x}S nanocrystals (NCs) were converted into monodisperse Cu_{2-x}S-Au₂S NCs of tunable composition, including pure Au₂S, by cation exchange. The near-infrared (NIR) localized surface plasmon resonance (LSPR) was damped and red-shifted with increasing Au content. Cu to Au exchange and vacancy filling occurred simultaneously. Partially exchanged Cu_{2-x}S/Au₂S core/shell structures evolved to dumbbell-like structures under electron irradiation in the transmission electron microscope (TEM).

Introduction

Cation exchange has attracted substantial attention as an effective means of synthesizing and modifying colloidal nanocrystals (NCs).¹⁻⁶ In a general cation exchange strategy, a template material (colloidal NCs) with a specific morphology and crystal structure is prepared, then metal complexes of the cations present in the target NC material, are reacted with the template NCs. These new cations diffuse into the NCs, as the original cations diffuse out, ultimately forming a new crystalline material that may or may not retain the crystal lattice structure and overall morphology of the template NCs.⁷⁻¹⁰ During the process of cation-exchange, the framework of the anion sublattice may be maintained or distorted depending on the size and the thermodynamic stability of the shapes of the original template colloidal NCs.⁴ The most commonly used template materials are cadmium chalcogenide colloidal NCs including cadmium sulfide (CdS)^{1, 2, 11-14}, cadmium selenide (CdSe)^{4, 8, 15-17}, cadmium telluride (CdTe)^{18, 19}, silver selenide (Ag₂Se)²⁰, and silver telluride (Ag₂Te)²¹, for which methods of preparing extremely high-quality monodisperse NCs of various shapes are well-developed. Cation exchange produced changes in the optical and electronic properties, typically a change of photoluminescence (PL) in these semiconductor NCs or quantum dots (QDs). This change allows for easy monitoring of the cation-exchange process and facilitates studies of the mechanisms of the exchange reactions without the use of transmission electron microscopy (TEM). Recently, a new class of self-doped semiconductor NCs with localized surface plasmon resonance (LSPR) has emerged as an important class of new nanomaterials.^{22, 23} In the present context, these materials allow us to study the cation-exchange reaction by monitoring the evolution of LSPR of such self-doped semiconductor NCs when

they are used as the template NCs.

Here, we demonstrate the use of self-doped copper sulfide (Cu_{2-x}S) NCs as a template for preparing gold sulfide (Au₂S) NCs by cation exchange. Such high-quality colloidal Au₂S NCs are difficult to prepare directly. Moreover, the Au³⁺ ion has relatively high electron affinity, often resulting in reduction of Au metal onto semiconductor NCs to form heterogeneous NCs rather than cation exchange.^{24, 25} The self-doped Cu_{2-x}S NCs employed here exhibit strong near infrared (NIR) LSPR due to the presence of copper vacancies and the associated high concentration of free holes in these NCs. This allows us to monitor and analyse the cation-exchange reaction in a manner comparable to studies of evolution of PL in QDs during cation exchange. Very recently, copper selenide (Cu_{2-x}Se) NCs were investigated as a template to synthesize semiconductor NCs including CdSe and ZnSe by cation-exchange.¹⁵ Herein, we show that Cu_{2-x}S is another very promising template material for cation-exchange reactions, especially for synthesizing Au₂S metal sulfide NCs which are rarely synthesized directly in solution, and are also difficult to produce by cation exchange using other template materials. Bulk Au₂S is a p-type semiconductor.²⁶ Au₂S nanostructures have been much less studied than the analogous Ag₂S and Cu₂S nanostructures, but can be expected to have similar potential for applications in sensors²⁷, optoelectronics²⁸, and photocatalysis²⁹. Cu_{2-x}S/Au₂S heterostructures may be even more interesting in this regard, but the band alignment between the two materials is not established, so specific properties and applications are difficult to predict. Nanostructures that combine Au₂S and Au have been proposed for use in theranostic applications.³⁰

Experimental Section

Chemicals. Copper(I) chloride (CuCl, 99.995%), oleylamine (OAm, 70%), oleic acid (OA, 90%), sulphur (S) powder (99.98%) and gold(III) chloride trihydrate (HAuCl₄·3H₂O, 99.9%) were purchased from Sigma Aldrich and were used without further purification.

Preparation of OA-S and Au precursors.

The OA-S precursor was prepared using a slight modification of methods we demonstrated previously.³¹ Typically, 1 mmol sulphur

powder was mixed with 10 mL oleic acid. Then the solution was heated to 120 °C and kept at this temperature for 1 h under nitrogen protection to produce a 0.1M OA-S precursor solution. Au precursor was prepared by fully dissolving 0.3 mmol HAuCl₄·3H₂O in a mixture of 3 mL OAm and 1 mL toluene via sonication for 20-30 min.

Synthesis of Cu_{2-x}S NCs

Cu_{2-x}S NCs were synthesized by the method we demonstrated previously. In a typical synthesis, 0.5 mmol CuCl was mixed with 10 mL OAm and the solution was degassed at 110 °C for 30 min to remove oxygen and water. Then the solution was heated to 205 °C and it turned transparent and yellow, indicating formation of organo-copper precursor in OAm. Then the temperature was reduced to 120 °C and 5 mL OA-S precursor was quickly injected into the solution. After injection, the solution was kept at 108 °C for another 1.5 min for growth of NCs. About 15 to 20 mL ethanol was added into the solution and the NCs were collected by centrifuging at 8000 rpm (about 8000 G) for 1 min. As-collected Cu_{2-x}S NCs were redispersed in chloroform. Ethanol was added into the dispersion again and Cu_{2-x}S NCs were collected by centrifugation. The final Cu_{2-x}S NCs were dispersed in 1 mL chloroform for further use.

Sequential cation exchange from Cu_{2-x}S NCs to Au₂S NCs

To convert Cu_{2-x}S NCs to Au₂S NCs by cation exchange, Cu_{2-x}S NCs were mixed with Au precursor in OAm/toluene. Varying amounts of Au precursor (750 μL, 2 mL, 3 mL, 4 mL containing 0.056, 0.150, 0.225, and 0.300 mmol Au, respectively) were mixed with 6 mL toluene, 3 mL OAm and 450 μL Cu_{2-x}S NP dispersion. Neglecting losses of Cu during Cu_{2-x}S NP synthesis and purification, this preparation would contain an estimated 0.225 mmol Cu. Thus, the ratio of Au added to the Cu used in preparing the NPs was 1:4, 2:3, 1:1, and 4:3 for addition of 750 μL, 2 mL, 3 mL, and 4 mL of Au precursor, respectively. The mixture was stirred vigorously and heated to 55 °C in a three-necked, round-bottomed flask for 55 min under nitrogen protection. After allowing the product to cool to room temperature, ethanol was added to flocculate the NPs, then the product NCs were collected by centrifuging at 9000 rpm (about 9000 G) for 1 min. The NCs were re-dispersed in chloroform then collected by centrifugation twice to adequately remove unreacted ligands before further characterization.

Characterization

Transmission Electron Microscopy (TEM). The size and

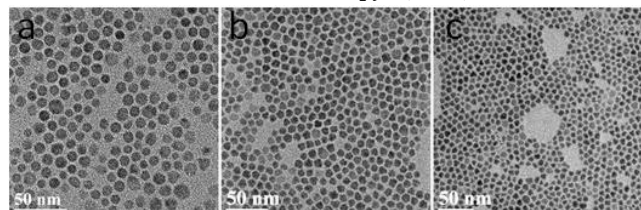


Figure 1. TEM images of (a) Cu_{2-x}S NCs used as templates, (b) Cu_{2-x}S-Au₂S NCs produced by cation exchange using 0.056 mmol Au precursor (nominal 1:4 Au:Cu ratio), and (c) Au₂S NCs produced by cation exchange using 0.3 mmol Au precursor (nominal 4:3 Au:Cu ratio).

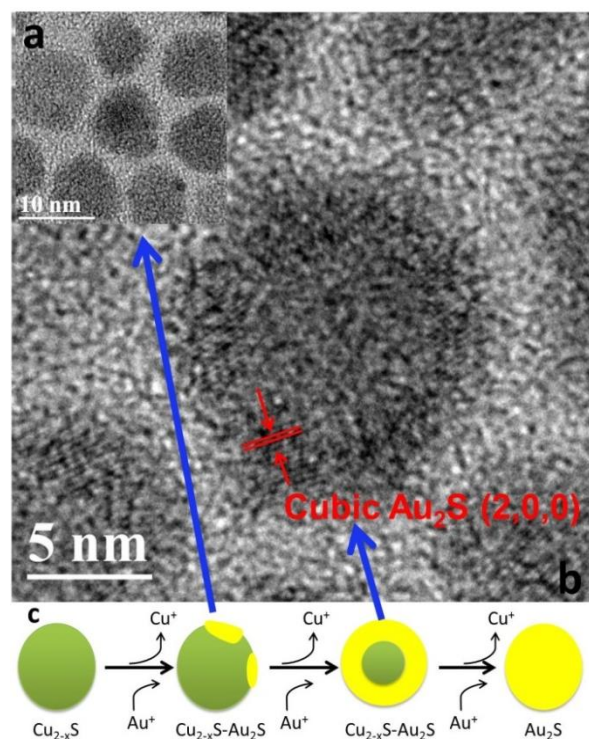


Figure 2. HRTEM images of NCs obtained after (a) cation exchange using 0.056 mmol Au precursor (nominal 1:4 Au:Cu ratio), and (b) cation exchange using 0.225 mmol Au precursor (nominal 1:1 Au:Cu ratio); (c) schematic illustration of the cation exchange process.

morphology of Cu_{2-x}S, Cu_{2-x}S-Au₂S and Au₂S NCs were characterized using a JEOL JEM-2010 microscope at a working voltage of 200 kV.

Energy Dispersive X-Ray Spectrometry (EDS). Elemental analysis of Cu_{2-x}S-Au₂S and Au₂S NCs was obtained using an Oxford Instruments X-Max 20 mm² energy dispersive x-ray spectroscopy detector within a Zeiss Auriga scanning electron microscope (SEM).

Powder X-Ray Diffraction (XRD). The crystal structures of Cu_{2-x}S, Cu_{2-x}S-Au₂S and Au₂S NCs were determined by XRD using a Bruker Ultima IV diffractometer with Cu K α x-ray source. Samples were prepared by drop-casting concentrated NCs dispersions onto glass slides.

UV-Vis-NIR Spectroscopy. Optical absorption spectra of Cu_{2-x}S, Cu_{2-x}S-Au₂S and Au₂S NC dispersions were measured using a Shimadzu 3600 UV-visible-NIR scanning spectrophotometer.

Results and Discussion

Cu_{2-x}S NCs were prepared via a slight modification of our previously reported method.³¹ Separately, Au precursor was prepared by dissolving auric chloride in a mixture of OAm and toluene. The cation exchange proceeded at relatively low temperature upon directly mixing the Cu_{2-x}S NCs and Au precursor

Table 1. EDS analysis of NCs produced by cation exchange

Au-precursor supplied (mmol)	Nominal Au:Cu ratio	EDS Analysis (mean atom percent)		
		Au	Cu	S
0.000	0	0.0	53.6	46.4
0.056	1:4	18.4	38.3	43.3
0.150	2:3	36.4	25.2	38.5
0.225	1:1	53.8	8.1	38.1
0.300	4:3	64.5	0.0	35.5

with sonication. TEM revealed that the Cu_{2-x}S NCs have a quasi-spherical shape and a size of 8.0 ± 0.9 nm (Fig. 1a). After cation exchange, the morphology and size of Cu_{2-x}S - Au_2S NCs did not change significantly, indicating that this process preserved the size and morphology of the template. When 0.3 mmol Au precursor was added to induce complete cation exchange, the size of product was 9.1 ± 0.8 nm (Fig. 1c) which was slightly larger than the template Cu_{2-x}S NCs. Figure 2a shows a high resolution TEM (HRTEM) of Cu_{2-x}S partially exchanged with Au ions. It reveals the formation of Au_2S nanocrystal domains on the Cu_{2-x}S NC surface and indicates the chemical transformation occurring from NC surface to core. HRTEM imaging of lattice planes in the layer coating the Cu_{2-x}S domain gave a lattice spacing of 0.25 nm, corresponding to the {200} planes of cubic Au_2S (Fig. 2b).

EDS analysis shows that the elemental ratio between Cu and S in the original Cu_{2-x}S particles is much less than 2:1, confirming the expected copper deficiency in the Cu_{2-x}S NCs. After cation exchange, the morphology and size of NCs did not show any obvious change, just a slight increase in size, suggesting that Au ions replace the original Cu ions within the NCs. EDS analysis clearly revealed the change in elemental fraction with the extent of cation-exchange (Table 1), as controlled by the amount of Au precursor provided. The elemental fraction of Au in the final Cu_{2-x}S - Au_2S NCs increased linearly with increasing amount of Au precursor employed in cation exchange process, while the Cu decreased almost linearly (Fig. 3). Ultimately, when 0.3 mmol Au precursor was used, the Cu ions were completely substituted by Au ions and pure Au_2S NCs were formed. Moreover, we observed that

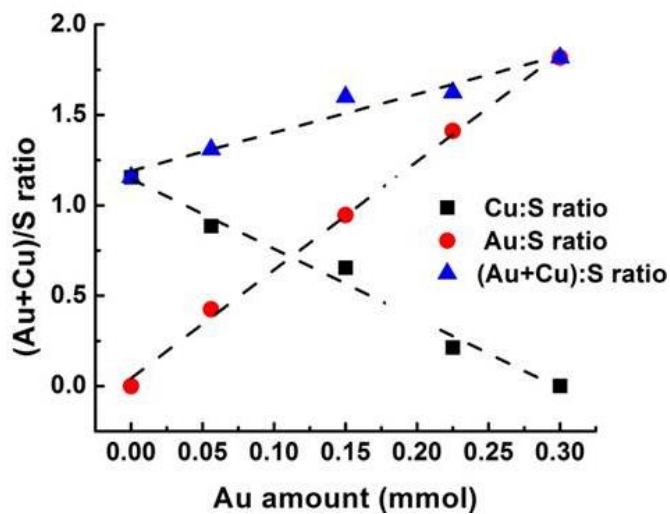


Figure 3. Dependence of copper, gold, and total cation content (relative to sulphur content) on the amount of Au precursor provided.

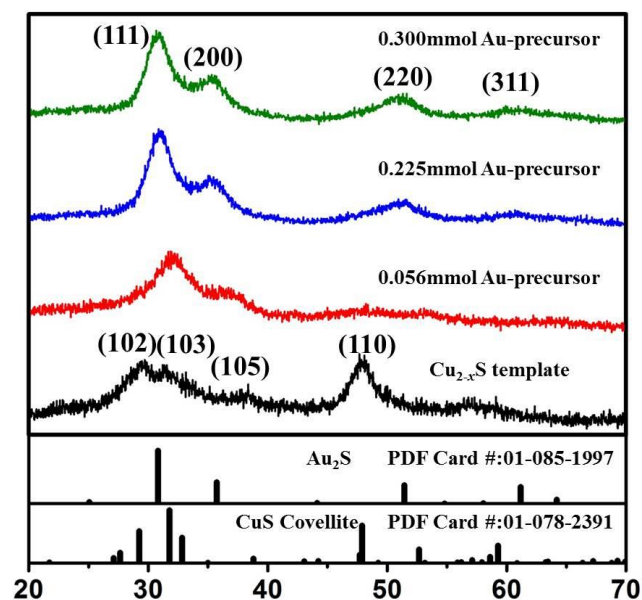


Figure 4. Evolution of crystal phases from Cu_{2-x}S to Au_2S crystal phases. The black curve shows the crystal phase of Cu_{2-x}S . The red and blue curves show the mixed crystal phases of Cu_{2-x}S - Au_2S prepared using 0.056 mmol Au (nominal 1:4 Au:Cu ratio) and 0.225 mmol Au (nominal 1:1 Au:Cu ratio). The green curve shows the crystal phase of Au_2S prepared using 0.300 mmol Au (nominal 4:3 Au:Cu ratio).

final Au:S elemental ratio was close to 2:1. This demonstrates that copper vacancies in the template nanoparticles (Cu_{2-x}S with x near 0.84) were eliminated and a new compound, Au_2S was formed through cation exchange. Thus, two processes must occur during the cation exchange: substitution of the Cu ions by Au ions and filling of the original cation vacancies by Au ions. The question of whether these two steps occur simultaneously or sequentially during cation exchange thus naturally arises. EDS analysis shows that cation vacancy concentration decreased gradually with increasing Au content in the final Cu_{2-x}S - Au_2S NCs, as demonstrated by the overall cation vs anion ratio ($(\text{Au}+\text{Cu}):(\text{S})$) plotted in Fig. 3. Note that, according to the EDS results, each Cu atom is replaced by roughly 1.2 Au atoms during the whole cation-exchange process, which indicates that substitution of Cu cations by Au cations and filling of cation vacancies occur simultaneously. Otherwise, the cation vacancy should decrease either before or after the Cu ions are significantly substituted by Au ions. In fact, the process of substituting Au atoms for Cu atoms in the lattice offers an opportunity for lattice reconstruction during cation exchange. In the process of this lattice rearrangement, Au ions also fill the cation vacancies. Although one might expect that the filling of copper vacancies by Au ions would be energetically preferable to replacing Cu ions with Au ions, simply filling vacancies in the Cu_{2-x}S lattice with Au ions without reconstruction, would lead to significant lattice expansion due to much larger ionic radius of Au compared to Cu. The increase in Gibbs free energy due to lattice expansion may be greater than the decrease due to vacancy filling, such that vacancy filling does not occur alone. Instead, cation exchange, vacancy filling, and lattice reconstruction appear to occur simultaneously, propagating across each nanocrystals from points on the exterior as illustrated in Figure 2.

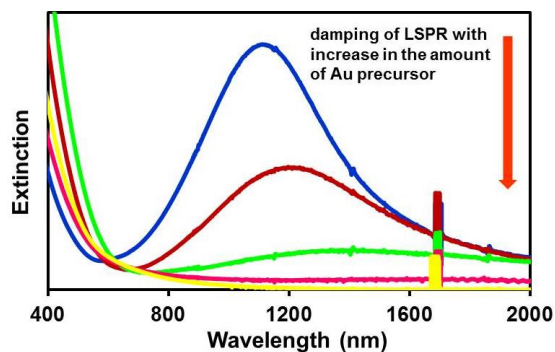


Figure 5. Optical extinction spectra illustrating LSPR of template Cu_{2-x}S NCs (blue) and cation-exchanged NCs following reaction using 0.056 (red), 0.150 (green), 0.225 (pink) and 0.300 (yellow) mmol Au precursor corresponding to Au:Cu ratios of 1:4, 2:3, 1:1, and 4:3, respectively.

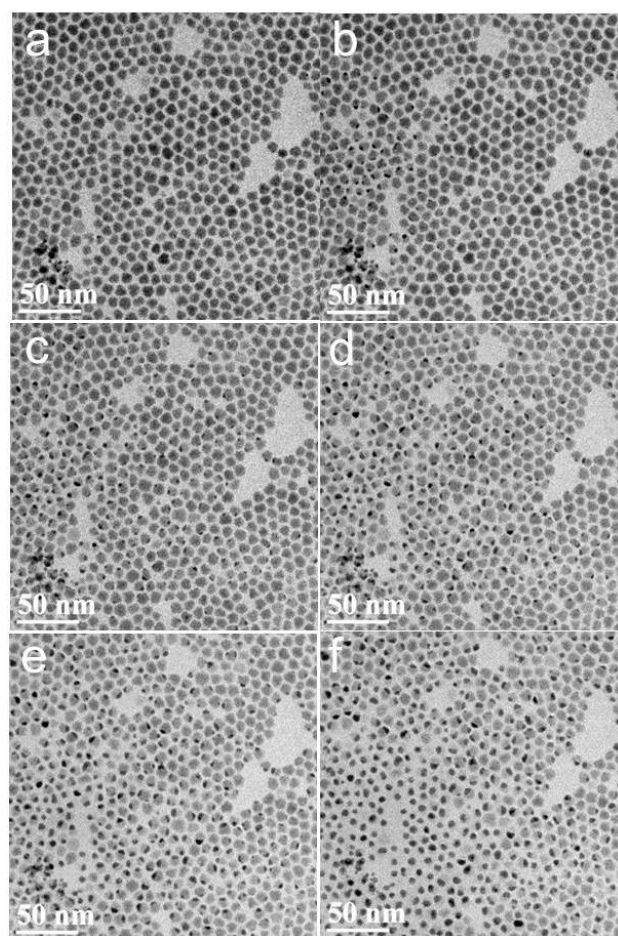


Figure 6. Stills of TEM recording of morphological transformation of $\text{Cu}_{2-x}\text{S}/\text{Au}_2\text{S}$ core/shell structure upon electron irradiation. Au_2S domains had merged together. (a) Initial configuration of $\text{Cu}_{2-x}\text{S}/\text{Au}_2\text{S}$ core/shell structure. (b)-(f) $\text{Cu}_{2-x}\text{S}@/\text{Au}_2\text{S}$ evolved to Au_2S -tipped Cu_{2-x}S nanoparticles. The stills were 15s time intervals: the total duration is 90s.

exhibited morphology evolution under electron beam irradiation in the TEM (**Fig. 6**). A systematic study of this shape evolution of the $\text{Cu}_{2-x}\text{S}-\text{Au}_2\text{S}$ NPs was carried out in the TEM under electron irradiation at a working voltage of 200 kV. TEM images taken at sequential time points (**Figure 6a-f**) clearly show the time-dependent morphology change of the $\text{Cu}_{2-x}\text{S}-\text{Au}_2\text{S}$ NPs. Initially, $\text{Cu}_{2-x}\text{S}/\text{Au}_2\text{S}$ core/shell structures were formed by partial cation-exchange. With increasing exposure to the electron beam, high-contrast dots started appearing on the side of the NPs. Both the size and number of the NPs with these dots increased with exposure time. The morphological transformation of hetero-

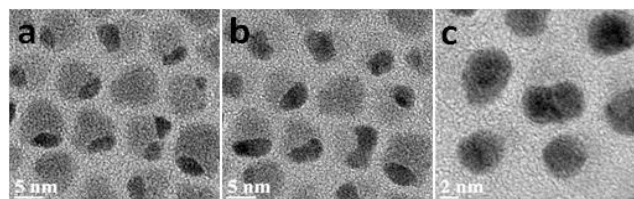


Figure 7. HRTEM images of $\text{Cu}_{2-x}\text{S}/\text{Au}_2\text{S}$ structural transformation under electron beam irradiation.

Powder XRD clearly shows the evolution of crystal phase following cation exchange using different amounts of Au precursor. The initial Cu_{2-x}S NCs have a hexagonal crystal structure (**Fig. 4**, black curve) that is consistent with the P63/mmc space group of covellite (CuS) and high chalcocite (Cu_2S). This pattern can be well fit to a mixture of these two hexagonal phases (**Fig. S2**). The diffraction peaks of the cubic Au_2S crystal phase appear upon cation exchange using 0.056 (red curve, nominal 1:4 Au:Cu ratio) mmol Au. With continuous increase in the amount of Au precursor, the diffraction intensity of peaks corresponding to the Au_2S crystal phase increase while diffraction peaks arising from the Cu_{2-x}S template disappear. In addition, the diffraction peaks shifted to lower angles with increasing Au content, reflecting an increase in the lattice constant. The hexagonal Cu_{2-x}S NCs fully evolved to cubic Au_2S NCs when 0.3 mmol Au precursor was used for cation exchange. These results are consistent with the EDS analysis in which very little Cu signal could be detected after cation exchange using 0.3 mmol Au precursor. Note that in the cation exchange process studied here, the producing NCs do not inherit the original crystal structure of the templating NCs.

Localized surface plasmon resonance has recently been observed and studied in copper-deficient copper chalcogenide NCs. Here, we focus on studying the evolution of LSPR of Cu_{2-x}S NCs during cation exchange with Au ions. The original Cu_{2-x}S NCs exhibit a LSPR peak centered at 1100 nm (**Fig. 5 blue curve**). Following partial cation exchange using a small amount of Au precursor (0.056 mmol, nominal 1:4 Au:Cu ratio), the plasmonic peak red-shifted 110 nm and obviously broadened (**Fig. 5 red curve**). This phenomenon is attributed to the dramatic decrease in the concentration of free holes as the cation vacancies are partially filled by Au ions in the NCs. Further damping and red shift of the LSPR was observed in the NPs prepared using 0.150 mmol Au precursor (nominal 2:3 Au:Cu ratio, green curve) and became negligible when 0.225 mmol or more Au precursor was used. The change of LSPR is consistent with the EDS analysis shown and discussed above.

Interestingly, we observed a morphology change when observing the partially ion-exchanged $\text{Cu}_{2-x}\text{S}-\text{Au}_2\text{S}$ nanostructures under TEM. This observation is qualitatively similar to that observed in heterogeneous NCs reported by other groups. For example, Huis *et al.* reported that CdS/Au nanorods transformed into AuS/Cd upon exposure to the electron beam in the TEM.³² Here, we observed that the partially ion-exchanged $\text{Cu}_{2-x}\text{S}-\text{Au}_2\text{S}$

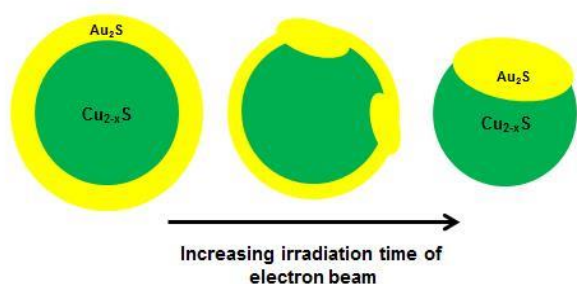


Figure 8. Schematic illustration of the apparent mechanism of morphological transformation of a $\text{Cu}_{2-x}\text{S}/\text{Au}_2\text{S}$ core/shell NC to a Au_2S -tipped Cu_{2-x}S NC by electron irradiation.

structures is more easily visible in HRTEM images (**Figure 7**). They clearly show growth and merging of the Au_2S domains from the image in **Fig. 7a** to that in **Fig. 7b**. Unfortunately, clear images of the original core/shell structures were not readily obtained; exposure sufficient to obtain good HRTEM images led to rapid transformation. A schematic illustration of the morphological evolution of hetero-structures is presented in **Figure 8**. Selected area electron diffraction (SAED) was used to determine the crystal phases of these two crystal domain. The mixed diffraction patterns (**Fig S3**) revealed the presence of two crystal domains corresponding to Cu_{2-x}S and Au_2S indicating that no new components such as Au or Cu nanocrystals were formed under electron beam irradiation. This result differs from the previously-reported observation in Au-tipped CdS nanorods in which new phases (Au_2S and Cd) were formed. In the present case, no new compound or crystal phases could be detected. Thus, we concluded that the morphology evolution from core/shell to dimer structures was mainly induced by the effect of thermal annealing due to the high energy of electron beam. In fact, annealing of core/shell NPs resulting in formation anisotropic dimer structures have been observed and studied previously in hot colloidal synthesis.³³ The temperature is one essential factor to control the morphology of heterogeneous NPs such as metal-metal oxide NPs. The SAED pattern of pure Au_2S NCs synthesized using 0.300 mmol Au precursor for cation exchange is shown in **Fig. S3**, and is consistent with XRD results showing formation of pure Au_2S crystal phase. This conclusively demonstrates that the darker domains are Au_2S and not Au domains.

Conclusions

In summary, we studied synthesis of Au_2S NPs by cation exchange using Cu_{2-x}S NPs as templates. LSPR in the self-doped Cu_{2-x}S NPs was gradually eliminated as Cu ions were displaced by Au ions and, simultaneously, Cu vacancies were filled. EDS analysis shows that the cation vacancy concentration was significantly decreased during formation of Au_2S . The morphology evolution of core/shell $\text{Cu}_{2-x}\text{S}/\text{Au}_2\text{S}$ NPs to dimer-like structures was observed under electron-beam irradiation in the TEM. The observation indicates that the intermediate $\text{Cu}_{2-x}\text{S}/\text{Au}_2\text{S}$ core/shell NPs obtained by partial cation exchange are metastable. This work shows that self-doped Cu_{2-x}S NPs can be used as a templating material for cation exchange synthesis of Au_2S . The process of

cation exchange can be monitored by measuring the change of optical absorption, which provides a facile way to systematically study the kinetics of cation exchange.

Acknowledgements

This work was partially supported by the New York State Center of Excellence in Materials Informatics.

Notes and references

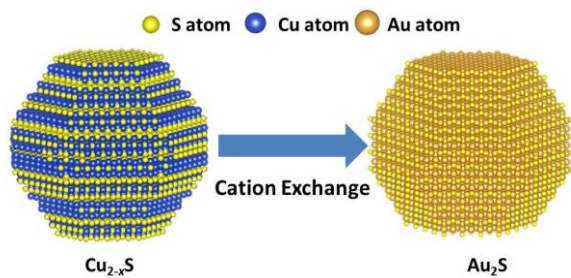
^a Department of Chemical and Biological Engineering, University at Buffalo (SUNY), Buffalo, New York, 14260-4200, USA; e-mail: swihart@buffalo.edu

Electronic Supplementary Information (ESI) available: Fig. S1, size distributions of NPs; Fig. S2, fit of XRD pattern of template NPs; Fig. S3, SAED patterns of NPs. See DOI: 10.1039/b000000x/

- R. D. Robinson, B. Sadtler, D. O. Demchenko, C. K. Erdonmez, L. W. Wang and A. P. Alivisatos, *Science*, 2007, **317**, 355-358.
- B. Sadtler, D. O. Demchenko, H. Zheng, S. M. Hughes, M. G. Merkle, U. Dahmen, L. W. Wang and A. P. Alivisatos, *J. Am. Chem. Soc.*, 2009, **131**, 5285-5293.
- J. M. Luther, H. M. Zheng, B. Sadtler and A. P. Alivisatos, *J. Am. Chem. Soc.*, 2009, **131**, 16851-16857.
- D. H. Son, S. M. Hughes, Y. Yin and A. P. Alivisatos, *Science*, 2004, **306**, 1009-1012.
- S. E. Wark, C. H. Hsia and D. H. Son, *J. Am. Chem. Soc.*, 2008, **130**, 9550-9555.
- J. B. Rivest and P. K. Jain, *Chem. Soc. Rev.*, 2013, **42**, 89-96.
- H. B. Li, R. Brescia, M. Povia, M. Prato, G. Bertoni, L. Manna and I. Moreels, *J. Am. Chem. Soc.*, 2013, **135**, 12270-12278.
- P. K. Jain, L. Amirav, S. Aloni and A. P. Alivisatos, *J. Am. Chem. Soc.*, 2010, **132**, 9997-9999.
- J. Park and S. W. Kim, *J. Mater. Chem.*, 2011, **21**, 3745-3750.
- B. J. Beberwyck and A. P. Alivisatos, *J. Am. Chem. Soc.*, 2012, **134**, 19977-19980.
- C. R. Lubeck, T. Y. J. Han, A. E. Gash, J. H. Satcher and F. M. Doyle, *Adv. Mater.*, 2006, **18**, 781-784.
- M. Saruyama, Y. G. So, K. Kimoto, S. Taguchi, Y. Kanemitsu and T. Teranishi, *J. Am. Chem. Soc.*, 2011, **133**, 17598-17601.
- B. Mukherjee, A. Peterson and V. Subramanian, *Chem. Commun.*, 2012, **48**, 2415-2417.
- J. M. Luther, H. Zheng, B. Sadtler and A. P. Alivisatos, *J. Am. Chem. Soc.*, 2009, **131**, 16851-16857.
- H. Li, M. Zanella, A. Genovese, M. Povia, A. Falqui, C. Giannini and L. Manna, *Nano Lett.*, 2011, **11**, 4964-4970.
- K. Miszta, D. Dorfs, A. Genovese, M. R. Kim and L. Manna, *ACS Nano*, 2011, **5**, 7176-7183.
- Z. H. Sheng, D. H. Hu, P. F. Zhang, P. Gong, D. Y. Gao, S. H. Liu and L. T. Cai, *Chem. Commun.*, 2012, **48**, 4202-4204.
- C. Chen, X. W. He, L. Gao and N. Ma, *ACS Appl. Mater. Interfaces*, 2013, **5**, 1149-1155.
- M. Liu, H. M. Zhao, X. Quan, S. O. Chen and H. T. Yu, *Chem. Commun.*, 2010, **46**, 1144-1146.
- M. Y. Chen and Y. J. Hsu, *Nanoscale*, 2013, **5**, 363-368.
- A. K. Samal and T. Pradeep, *Nanoscale*, 2011, **3**, 4840-4847.
- A. Comin and L. Manna, *Chem. Soc. Rev.*, 2014, **43**, 3957-3975.
- X. Liu and M. T. Swihart, *Chem. Soc. Rev.*, 2014, **43**, 3908-3920.
- A. E. Saunders, I. Popov and U. Banin, *J. Phys. Chem. B*, 2006, **110**, 25421-25429.
- A. Figuerola, M. van Huis, M. Zanella, A. Genovese, S. Marras, A. Falqui, H. W. Zandbergen, R. Cingolani and L. Manna, *Nano Lett.*, 2010, **10**, 3028-3036.
- K. Ishikawa, T. Isonaga, S. Wakita and Y. Suzuki, *Solid State Ionics*, 1995, **79**, 60-66.
- D. S. Wang, C. H. Hao, W. Zheng, Q. Peng, T. H. Wang, Z. M. Liao, D. P. Yu and Y. D. Li, *Adv. Mater.*, 2008, **20**, 2628-2632.

-
28. Y. Jiang, X. Zhang, Q. Q. Ge, B. B. Yu, Y. G. Zou, W. J. Jiang, W. G. Song, L. J. Wan and J. S. Hu, *Nano Lett.*, 2014, **14**, 365-372.
29. Y. Liu, Y. H. Deng, Z. K. Sun, J. Wei, G. F. Zheng, A. M. Asiri, S. B. Khan, M. M. Rahman and D. Y. Zhao, *Small*, 2013, **9**, 2702-2708.
30. L. Ren, X. L. Huang, B. Zhang, L. P. Sun, Q. Q. Zhang, M. C. Tan and G. M. Chow, *J. Biomed. Mater. Res., Part A*, 2008, **85**, 787-796.
- 10 31. X. Liu, X. L. Wang, B. Zhou, W. C. Law, A. N. Cartwright and M. T. Swihart, *Adv. Funct. Mater.*, 2013, **23**, 1256-1264.
32. M. A. van Huis, A. Figuerola, C. Fang, A. Beche, H. W. Zandbergen and L. Manna, *Nano Lett.*, 2011, **11**, 4555-4561.
33. C. George, D. Dorfs, G. Berton, A. Falqui, A. Genovese, T. Pellegrino, A. Roig, A. Quarta, R. Comparelli, M. L. Curri, R. Cingolani and L. Manna, *J. Am. Chem. Soc.*, 2011, **133**, 2205-2217.
- 15

TOC Figure:



TOC sentence:

Self-doped Cu_{2-x}S plasmonic semiconductor nanocrystals were converted into monodisperse Cu_{2-x}S - Au_2S nanocrystals of tunable composition, including pure Au_2S , by cation exchange.